Artificial Enzyme-Powered Microfish for Water-Quality Testing

Jahir Orozco, Victor García-Gradilla, Mattia D'Agostino, Wei Gao, Allan Cortés, and Joseph Wang*

Department of Nanoengineering, University of California, San Diego, La Jolla, California 92093, United States

ABSTRACT We present a novel micromotor-based strategy for water-quality testing based on changes in the propulsion behavior of artificial biocatalytic microswimmers in the presence of aquatic pollutants. The new micromotor toxicity testing concept mimics live-fish water testing and relies on the toxin-induced inhibition of the enzyme catalase, responsible for the biocatalytic bubble propulsion of tubular microengines. The locomotion and survival of the artificial microfish are thus impaired by exposure to a broad range of contaminants, that lead to distinct time-dependent irreversible losses in the catalase activity, and hence of the propulsion behavior. Such use of enzyme-powered biocompatible polymeric (PEDOT)/Au-catalase tubular microengine offers highly sensitive direct optical visualization of changes in the swimming behavior in the presence of common contaminants and hence to a direct real-time assessment of the water quality. Quantitative data on the adverse effects of the various toxins upon the swimming behavior of the enzyme-powered artificial swimmer are obtained by estimating common ecotoxicological parameters, including the EC_{50} (exposure concentration causing 50% attenuation of the microfish locomotion) and the swimmer survival time (lifetime expectancy). Such novel use of artificial microfish addresses major standardization and reproducibility problems as well as ethical concerns associated with live-fish toxicity assays and hence offers an attractive alternative to the common use of aquatic organisms for water-quality testing.

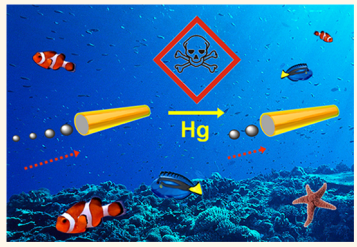

KEYWORDS: nanomotors · microfish · toxicity · propulsion · catalase · pollution

Pollution by aquatic contaminants is among the most challenging issues to our ecosystems and living environment. One of the oldest and most widely used approaches for testing the quality of our water resources relies on changes in the swimming behavior and lifetime expectancy of live fish in the presence of toxic substances.[1−3] Such monitoring of fish survival and performance provides qualitative and quantitative information about the quality of the water system. The main technical drawbacks associated with fish-toxicity assays are standardization problems of the organisms, lack of reproducibility, and the requirement for skilled operators.[4,5] In addition, there are growing ethical concerns and related regulations and costs that hinder live-fish lethal bioassays.

Here we demonstrate a novel nanotechnological alternative for assessing the water quality and indicating the presence of aquatic pollutants based on the use of enzyme-powered artificial "microfish". The motion of synthetic micromotors has received a considerable fundamental and practical interest over the past decade.[6−11] Bubble-propelled catalytic and biocatalytic tubular microengines have been particularly useful for various practical applications due to their efficient propulsion in various real-life media.[12−16] Biocatalytic layers, based on immobilized catalase, have been shown to be an attractive alternative to catalytic Pt metal layers for propelling such hydrogen-peroxide powered microengines.[17,18] Different practical micromotor applications, ranging from drug delivery,[19] to target isolation[20] and environmental remediation,[21,22] have thus been proposed.

The new microengine-based water toxicity testing relies on changes in the propulsion behavior associated with the inhibition of the catalase biocatalytic layer by common pollutants such as heavy metals, pesticides, and herbicides (Figure 1). Enzyme-based inhibition assays have been widely used for measuring toxins in diverse matrices based on the decreased biocatalytic activity that leads to lower optical or electrical signals.[23−27] The antioxidant activity of catalase has been suggested as a vital biomarker of fish intoxication when exposed to chemical pollutants.[28] In the following sections we will illustrate that well-defined changes in the swimming performance

* Address correspondence to josephwang@ucsd.edu.

Received for review November 19, 2012 and accepted December 12, 2012.

Published online December 12, 2012
10.1021/nn305372n

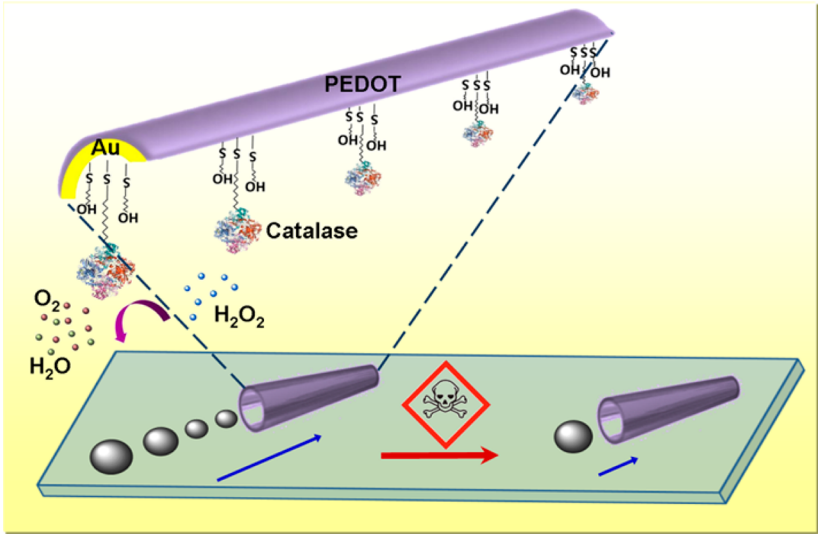

Figure 1. Scheme illustrating the pollutant effect on the microfish locomotion speed through inhibition of the catalase biocatalytic layer (bottom) along with the protocol used for immobilizing the enzyme at the inner gold surface of the tubular microengine through a mixed MUA/MCH self-assembled monolayer (top).

and lifetime expectancy (survival) of self-propelled biocatalytic microengines are observed in the presence of a wide variety of organic and inorganic contaminants known to inhibit the catalase activity.[23,29,30] Optical tracking of the movement of the artificial microfish thus offers a simple and direct visualization of these toxin-induced changes in the swimming performance. Such real-time tracking of changes in the swimming behavior of the artificial microfish has been illustrated upon exposure to model aquatic pollutants, including the heavy metals mercury and copper, the sodium-azide (NaN_3) pesticide and the aminotriazole herbicide, with the peroxide fuel acting also as the substrate of such motor-based inhibition assays. Copper and mercury are of special concern among metal pollutants, owing to their considerable toxicity to aquatic animals at relevant concentrations.[1] Quantitative assessment of the toxin-microswimmer effect is obtained by estimating ecotoxicological parameters, such as 50% exposure concentration effect (EC_{50}) and survival time (T_{50}), commonly used in live-fish water testing.[1] The observed trends in the EC_{50} and T_{50} values thus reflect the adverse effects of toxins upon the propulsion behavior and correlate well with their known inhibitory action.[1,30]

The new nanoswimmer water-toxicity assay strategy offers direct monitoring of aquatic contaminants down to the micromolar levels and addresses standardization and reproducibility problems and major ethical concerns associated with live-fish toxicity bioassays. Unlike live fish, artificial micromotors are not subject to differences in metabolic and excretion rates, or stress level, and can be mass-produced and functionalized in a highly reproduced fashion. This novel nanomachine-based toxicity assay approach thus represents an attractive environmentally friendly nanotechnological alternative to the common use of aquatic organisms for testing the quality of our water resources.

RESULTS

The artificial microfish were fabricated by a template-based electrodeposition of PEDOT/Au bilayer microtubes.[18] Such microfish have a defined conical microtube configuration, with a length of ~8 μm, outer diameters of 2.0 and 1.2 μm, along with inner openings of 1.6 and 0.8 μm.[13,18] Figure 1 depicts a layout of this synthetic nanoswimmer, illustrating the chemistry used for linking catalase to its inner gold surface along with a cross section of the microengine and the corresponding surface layers. The outermost polymeric tubular layer was prepared by electropolymerization of the EDOT monomer on the walls of the membrane micropores, followed by electrodeposition of the gold metallic layer. The enzyme was anchored to the gold layer *via* a common carbodiimide (EDC)/*N*-hydroxysuccinimide (NHS) chemistry through a mixed self-assembled binary monolayer of 11-mercaptoundecanoic acid (MUA)/6-mercaptohexanol (MCH) alkanethiols. The biocatalytic decomposition of the hydrogen peroxide fuel at the inner enzymatic layer of the microtube thus generates the oxygen bubble thrust and leads to an efficient swimming motion of the microfish. In the presence of chemical stress (*e.g.*, heavy metals, pesticides, and herbicides), such biocatalytic activity of catalase is inhibited, resulting in a lower bubble frequency and an impaired locomotion of the artificial microfish (Figure 1, bottom). Time-dependent optical tracking of changes in the microfish speed and of its lifetime (survival), thus provide useful information on the inhibitory activity and toxicity of the corresponding pollutants. Unlike earlier motion-based biosensing applications involving the attachment

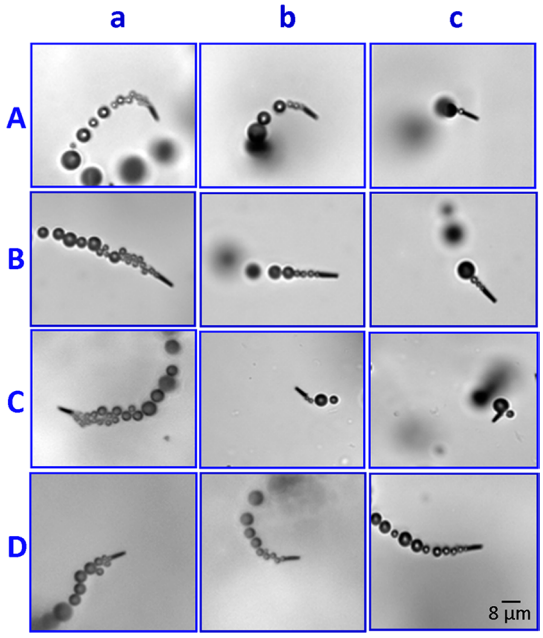

Figure 2. Toxin-induced changes in the swimming behavior. Time-lapse images taken (from Supporting Information, videos 1, 2, and 3) over a 3 s period following (a) 0, (b) 2, and (c) 4 min exposures of the microengines to different water pollutants: (A) 0.2 mM Cu, (B) 25 μM NaN_3, and (C) 625 mM aminoriazole; (D) control (blank solution). Substrate/fuel concentration, 2% hydrogen peroxide.

of bioreceptors,[15,20] no additional surface functionalization is required for realizing the microfish-based water-quality testing.

The propulsion efficiency of artificial biocatalytic microswimmers depends on the influence of the toxin upon the activity of the enzyme powering the motor. The locomotion and survival of the artificial microfish are impaired by exposure to a broad range of contaminants *via* inhibition of the catalase activity. Such changes in the movement of the microfish can be readily visualized and tracked in real time using optical microscopy videos and images. The 8-μm length of our biocatalytic microengines thus offers a convenient visualization of these swimmers and direct tracking of the toxin-induced changes in the propulsion behavior. Such changes in the swimming performance and lifetime expectancy of microfish were evaluated by using model pollutants, representative of heavy metals, pesticides, and herbicides contaminants.

The attenuated motion of the artificial microfish in the presence of these pollutants is clearly indicated by observing changes in the ejection of oxygen bubbles (from the tail end of the microfish) that are responsible for its efficient propulsion. For instance, Figure 2 displays time-lapse images (taken from Supporting Information, videos 1, 2, and 3) illustrating changes in the microfish locomotion in the presence of three common contaminants. These images were recorded over a 3 s period following 0 (a), 2 (b), and 4 (c) min exposures to 0.2 mM Cu (A), 25 μM NaN_3 (B), and

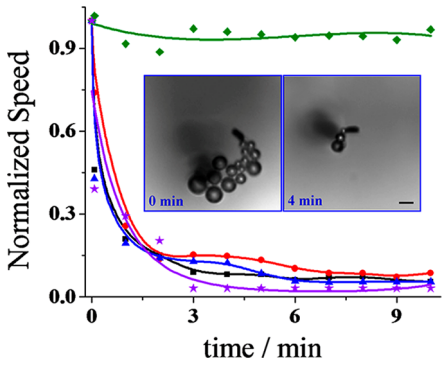

Figure 3. Changes in the swimming behavior of the artificial microfish as a function of time upon exposure to 100 μM Hg (black square), 0.6 mM Cu (purple stars), 25 μM sodium azide (red circle), 625 mM aminotriazole (blue triangle), and a control experiment without the toxins (green diamond). Curves were plotted by tracking the normalized microfish speed after exposure to the pollutants. Inset: time-lapse images of the microfish recorded after 0 and 4 min swimming in a 100 μM Hg solution. Scale bar, 6.0 μm.

625 mM aminotriazole (C). For example, navigation in the 0.2 mM copper solution resulted in a sharp decrease in the number of oxygen bubbles (observed during this 3 s period) from ~20 to 7 and 2 following 2 and 4 min exposures, respectively (A). Similar changes in the bubble frequency and propulsion efficiency are observed following 2 and 4 min movement in the 25 μM NaN_3 (B) and 625 mM aminotriazole (C) solutions. The corresponding videos (Supporting Information, videos 1, 2, and 3) clearly illustrate the reliable real-time tracking of the changes in the swimming performance, including the diminished bubble ejection and greatly reduced speed in the presence of these chemicals. A dramatic change in the swimming behavior is thus observed after the 2 min exposure, with a nearly complete attenuation of the movement indicated following the 4 min exposure. However, no apparent change in the trajectory of the microswimmers accompanies these changes in the enzymatic activity.

Figure 3 displays a comparative study of the changes in the propulsion behavior of the catalase-based microengine over a 10 min period in the presence of 4 common contaminants: mercury (black), sodium azide (red), aminotriazole (blue), and copper (purple). To account for the broad range of the toxicity of these contaminants and monitoring significant changes within the same short time scale, the level of these pollutants was adjusted to 100 μM Hg, 0.6 mM Cu, 25 μM sodium azide, and 625 mM aminotriazole. These toxin levels lead to a rapidly diminished propulsion efficiency with speed diminutions of about 70−75%, 80−85%, and 90−95% within 1, 2, and 6 min exposures to these contaminants, respectively. For example, the presence of 0.6 mM Cu leads to a 95% diminution of the microfish speed within 4 min. A nearly complete loss of the swimming ability is thus observed in the presence of the four chemicals within the experimental

time scale. In contrast, no apparent change in the propulsion behavior is observed during the same period in the absence of toxins (green, control experiment). Also shown in Figure 3 (inset), are time-lapse images of the microfish locomotion (taken from Supporting Information, video 4) before and after a 4 min navigation in the mercury solution. These images illustrate substantially fewer ejected oxygen bubbles following such exposure to mercury.

The substrate concentration has been shown to affect the degree of enzymatic inhibition.[23] Enzyme inhibition assays, particularly those involving noncompetitive inhibition, often rely on operation with high (saturating) substrate concentrations.[27] Using the present catalase-powered microengines, the peroxide fuel is acting also as the substrate for the microfish-based toxicity (inhibition) assay. The substrate saturation conditions were estimated by measuring changes in the microfish speed (signal) upon an increase in the peroxide concentration. Supporting Information, Figure 2 shows such dependence, and fit with the Michaelis–Menten behavior, with the reaction reaching its maximal velocity (V_{max}) at peroxide levels higher than 2%. A 2% hydrogen peroxide fuel level was thus selected as the working substrate concentration for comparing the effect of the different pollutants on the microfish behavioral response. As indicated from Supporting Information, Figure 2, the presence of inhibitor did not affect the hyperbolic profile of the speed-signal *vs* substrate-concentration dependence of the catalase-based microengine but influenced the V_{max}. For example, V_{max} decreased by nearly 50% in the presence of Cu (Supporting Information, Figure 2). The trend and the change in V_{max} indicate the noncompetitive inhibition effect of Cu, in agreement with an early report.[1] A similar trend was observed in the presence of mercury (not shown).

Major drawbacks associated with live-fish toxicity assays are standardization problems of the organisms, lack of reproducibility, and the requirement for skilled operators.[4,5] To ensure reproducible results, the live fish used should be from the same source and of the same age. In contrast, the membrane template preparation of our artificial microtube swimmers leads to highly reproducible microengines and propulsion behavior.[13,18] The reproducibility and stability of the new microfish-based water-quality testing approach were investigated by tracking the movement of multiple swimmers from the same batches and from different batches, following identical motor fabrication and surface-modification procedures. The results demonstrated highly reproducible propulsion behavior among different microfish in both unpolluted and polluted water samples. For example, a series of measurements involving 10 different batches of swimmers (and 5 swimmers from each batch) displayed a reproducible initial speed of 54.0 $\pm$ 3.5 μm/s. Such speed decreased to 32.6 $\pm$ 4.1 μm/s after a 10 s exposure to a 5 μM Hg solution. The initial speed of the catalase-powered microengines remained constant for up to one week from their preparation (with variations lower than 10%), thus demonstrating their stability and potential use as reliable long-term pollution indicator.

TABLE 1. Summary of the Microfish Toxicity Indicators Data for the Individual Pollutants Tested[a]

pollutant	range tested	EC_{50}	EC_{90}	T_{50}, s	T_{90}, s
Hg	5.0–200 μM	50 μM	100 μM	15	180
Cu	0.2–1.0 mM	0.2 mM	0.6 mM	24	135
NaN_3	2.5–25 μM	2.5 μM	25 μM	33	375
Aminotriazole	375–750 mM	375 mM	625 mM	12	276

[a] The EC_{50} and EC_{90} ecotoxicological indicators are defined as the concentration of contaminant that is able to produce a 50% and higher than 90% attenuation of microfish locomotion in 2 and 10 min, respectively. T_{50}, time taken for the microfish speed to decrease 50% (relative to the initial one in the presence of inhibitor at EC_{90}).

Analogous to the common use of LD_{50} in live fish toxicity testing,[2] IC_{50} is used in enzyme-inhibition assays to estimate the inhibitor concentration leading to a 50% enzymatic inhibition, while EC_{50} is used as the ecotoxicological parameter assessing the behavioral response.[1] Herein we define EC_{50} and EC_{90} as the contaminant concentrations leading to 50% and 90% attenuation of the nanomotor locomotion within 2 and 10 min, respectively. Table 1 summarizes the experimental EC_{50} and EC_{90} values obtained for the catalase-powered microengine. Sodium azide displayed the lower EC_{50} value (2.5 μM), followed by Hg, Cu, and aminotriazole with 50% speed decays at 50 μM, 0.2 mM, and 375 mM, respectively. The EC_{90} values are 25 μM, 100 μM, 0.6 mM, and 625 mM for NaN_3, Hg, Cu and aminotriazole, respectively. Furthermore, we define T_{50} as the time taken for the microfish speed to decrease by 50% (from the initial one) in the presence of the inhibitor at EC_{90}. T_{50} values of 12, 15, 24, and 33s have thus been estimated for aminotriazole, Hg, Cu, and NaN_3, respectively. The extremely short analysis times of the artificial microfish approach (from a few seconds to 10 min), compared to 24–92 h for conventional live-fish toxicity assays,[1] make the new nanomotor strategy extremely attractive for rapid screening of water pollution and hazards.

Figure 4 presents the behavior response of the artificial microfish after a 2 min exposure to different concentrations of heavy metals (a), pesticides, and herbicides (b). The corresponding videos are included as Supporting Information videos 1–4. Both mercury and copper display a dramatic effect upon the microfish swimming behavior, with a substantial and rapid speed diminution of nearly 80% at 50 μM Hg and 300 μM Cu, followed by a leveling off up to 140 μM Hg and 600 μM Cu, and a nearly complete (~95%) attenuation of the movement around 210 μM Hg and

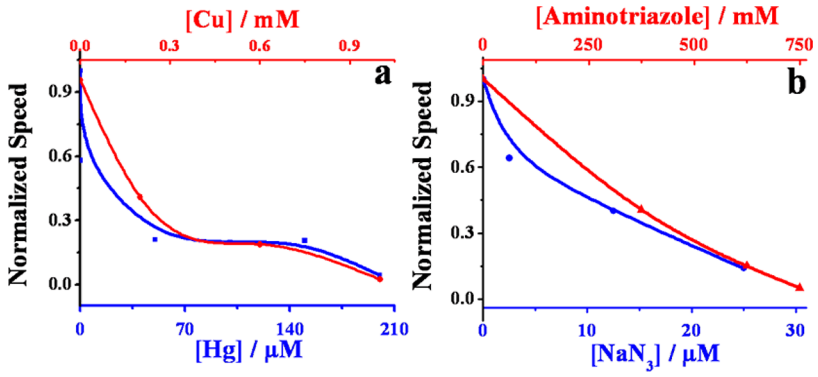

Figure 4. Effect of the pollutant concentration upon the swimming performance of the microfish, as indicated from changes in the locomotion speed after a 2 min exposure. (a) Influence of the metals Hg (blue) and Cu (red) over the 0.05−0.20 mM and 0.2−1.0 mM ranges, respectively. (b) Influence of NaN_3 (blue) and aminotriazole (red) over the 2.5−25 μM and 375−750 mM ranges, respectively.

1000 μM Cu (Figure 4a and Supporting Information videos 1 and 4). These results indicate that Hg is producing a similar effect on the microfish swimming performance as Cu does at 4−6 fold higher concentrations. This is in agreement with live-fish bioassays that display a higher effect of Hg on the lethargic and erratic swimming behavior of live fish, compared to Cu, starting within 48 h exposure to 100 μg/L Hg and 800 μg/L Cu, respectively.[1] The most widely reported ecologically sensitive parameter has been the swimming distance in the presence of the EC_{50} levels of 1.2 and 12.3 μg/L for Hg and Cu, respectively.[1] Figure 4b (and Supporting Information videos 2 and 3) illustrate the effect of NaN_3 pesticide and aminotriazole herbicide by varying their levels from 2.5 to 25 μM (NaN_3) and from 375 to 750 mM (aminotriazole). A similar behavioral response is observed for these pollutants with a gradual decrease of the original speed by up to 15% at around 25 μM NaN_3 and 625 mM aminotriazole, respectively. Yet, NaN_3 displays the stronger effect upon the swimming behavior of the microfish, considering its greatly lower concentration range.

Measurements of the life expectancy of the artificial microfish were further used to evaluate its behavior response in the presence of common contaminants. To assess the life expectancy of the artificial swimmer, we defined the survival time as the time period from the initial exposure to a given toxin concentration taken for the microfish to lose its directional movement and reach its minimal speed. Figure 5 displays the dependence of the survival time of the microfish upon the concentration of the different pollutants. As expected, the survival time is strongly dependent upon the level of these contaminants, for example, decreasing rapidly from 6 min to 30 s upon raising the mercury concentration from 50 to 200 μM. Different concentration ranges were used for the different pollutants, reflecting their broad range of toxicities. In all cases, the microfish survival time is lower than 10 min, with the shortest time of 10 s observed for 750 μM aminotriazole and

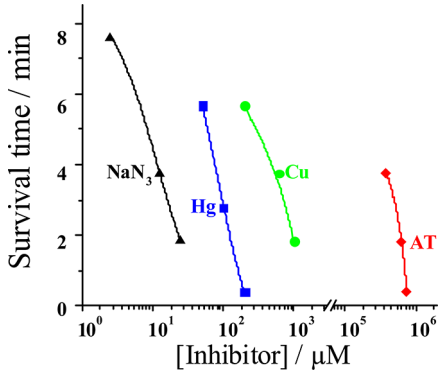

Figure 5. Dependence of the survival time of the artificial microfish upon the pollutant concentration (2.5−25 μM NaN_3, black; 50−200 μM Hg, blue; 0.2−1.0 mM Cu, green; and 375−750 mM aminotriazole (AT), red). Survival time is defined as the time it takes for the fish to lose its directional movement (and reaches its minimal speed).

200 μM Hg. Overall, the data of Figure 5 indicate that NaN_3 displays the strongest effect upon the survival time of the artificial microfish (with short survival times at lowest concentrations), followed by Hg, Cu, and aminotriazole.

CONCLUSIONS

We have presented a new simple and cost-effective nanotechnology strategy for water-quality testing based on changes in the propulsion behavior and lifetime of artificial biocatalytic microswimmers in the presence of aquatic pollutants, in a manner analogous to changes in the swimming behavior and survival of natural fish used for toxicity testing. Various model organic and inorganic pollutants have displayed a significant concentration-dependent effect upon the swimming behavior of the microfish swimmer. Such use of self-propelled artificial swimmers allows direct visualization (optical tracking) of the changes in the swimming behavior in response to the presence of chemical stress. Such changes in the swimming behavior reflect the inhibition of the biocatalytic layer

responsible for the bubble-propulsion thrust, and hence the toxin-induced hindered movement and life expectancy of these tubular microengines. Similar to the common use of live fish, the microfish water-quality testing involves changes in the propulsion behavior and lifetime of biocatalytic microengines. While various toxins display different effects upon the propulsion behavior (as common also in live-fish testing), the new microfish method does not offer a selective response, as expected for enzyme inhibition processes.[23] Other nontoxic compounds or salts are not expected to influence the movement of bubble-propelled microtubular engines.[13,15,31] The minimal salt effect[31] indicates suitability of the microfish for monitoring a variety of natural water systems with different ionic strengths. Self-driven millimeter-sized motors (based on changes in the surface tension), in contrast, display different speeds in the presence of organic solvents such as acetonitrile or *N,N′*-dimethylformamide.[22] The composition of our enzyme-powered polymer-based microengines[18] makes these microfish highly compatible and environmentally friendly. By addressing major drawbacks and ethical concerns associated with live-fish toxicity assays the new man-made nanomachine strategy offers an attractive alternative to the common use of aquatic organisms for water-quality testing.

EXPERIMENTAL SECTION

Preparation of the Artificial Microfish. Tubular microengines were prepared using a common template directed electrodeposition protocol.[18] A Cyclopore polycarbonate membrane, containing 2 μm diameter conical-shaped micropores (Catalog No 7060-2511; Whatman, Maidstone, U.K.), was employed as the template. A 75 nm-thick gold film was first sputtered on one side of the porous membrane to serve as the working electrode using the Denton Discovery 18 sputtering system. The coating was performed at room temperature under base vacuum of 5×10^{-6} Torr, DC power 200 W and Ar pressure of 3.1 mT, along with a rotation speed of 65 rpm and sputtering time of 90 s. A Pt wire and Ag/AgCl (3 M KCl) served as counter and reference electrodes, respectively. The membrane was then assembled in the electrochemical plating cell with an aluminum foil serving as a contact.

Poly(3,4-ethylenedioxythiophene) (PEDOT) microtubes were electropolymerized at +0.80 V using a charge of 0.06 C from a plating solution containing 15 mM EDOT, 7.5 mM KNO_3 and 100 mM sodium dodecyl sulfate (SDS); subsequently, gold was plated at −0.9 V for 1 C from a commercial gold plating solution (Orotemp 24 RTU RACK; Technic Inc.). Details of the various reagents have been described elsewhere.[18] The sputtered gold layer was completely removed by hand polishing with alumina slurry (3−4 μm). The membrane was then dissolved in methylene chloride for 10 min to completely release the microtubes. The latter were collected by centrifugation at 6000 rpm for 3 min and washed repeatedly with methylene chloride, followed by ethanol and ultrapure water (18.2 MΩ · cm), three times each, with a 3 min centrifugation following each wash. All microtubes were stored in ultrapure water at room temperature until use.

Immobilization of Catalase. The inner Au layer of the bilayer microtubes was functionalized first with a mixed MUA/MCH alkanethiol monolayer. A solution mixture of 2.5 mM MUA and 7.5 mM MCH was prepared in ethanol. The microtubes were incubated in the MUA/MCH solution overnight. After rinsing the tubes with water for 5 min, they were transferred to an eppendorf vial containing a 200 μL PBS buffer (pH 5.5) solution with the coupling agents 1-ethyl-3-[3-dimethylaminopropyl] carbodiimide hydrochloride (EDC), *N*-hydroxylsulfosuccinimide (Sulfo-NHS) at 0.4 and 0.1 M, respectively, and the catalase enzyme (2 mg/mL). This incubation was carried out for 7 h at 37 °C, followed by two 15 min rinsing steps with PBS solution (pH 5.5), containing 0.05 wt % SDS. Finally, the microengines were washed repeatedly by centrifugation at 6000 rpm for 3 min with water for three times to remove the excess of catalase from the solution, and were suspended in 5.5 pH buffer and stored at 4 °C until use.

Equipment. Template electrochemical deposition of microtubes was carried out with a CHI 661D potentiostat (CH Instruments, Austin, TX). An inverted optical microscope (Nikon Instrument Inc. Ti-S/L100), coupled with a 40× objective, a Photometrics QuantEM 512/SC camera (Roper Scientific, Duluth, GA) and MetaMorph 7.6 software (Molecular Devices, Sunnyvale, CA) were used for capturing movies at a frame rate of 30 frames per sec. The speeds of the microengines were tracked using a Metamorph tracking module and the results were statistically analyzed using Origin software.

Experimental Setup. Experiments were performed by casting equal volumes (~2.0 μL) of solutions containing microfish, sodium cholate (NaCh), and hydrogen peroxide solutions on a glass slide to obtain final concentrations of 5% NaCh and 2.0% H_2O_2. Once the movement of the artificial microfish was established, a dose of the target pollutant (containing also the same peroxide and NaCh levels) was added to obtain the desired concentration of pollutant. Movement of the microfish was recorded first in the unpolluted solution and subsequently after adding the contaminant for at least 10 min, in 1 min intervals.

Conflict of Interest: The authors declare no competing financial interest.

Supporting Information Available: Micromotor preparation, related protocols, instrumentation, reagents, additional data and videos. This material is available free of charge *via* the Internet at http://pubs.acs.org.

Acknowledgment. This project received support from the Defense Threat Reduction Agency-Joint Science and Technology Office for Chemical and Biological Defense (Grant No. HDTRA1-13-1-0002). J.O., V.G., and M. D'A. acknowledge financial support from the Government of Catalonia (a Beatriu de Pinós Fellowship), CONACYT Mexico and Italy, respectively. V.G. is on leave from UNAM-CNYN. W.G. is a Howard Hughes Medical Institute International Student Research fellow. The authors also thank C. Hennessy and A. Pourazary for their assistance.

REFERENCES AND NOTES

1. Vieira, L. R.; Gravato, C.; Soares, A. M. V. M; Morgado, F.; Guilhermino, L. Acute Effects of Copper and Mercury on the Estuarine Fish Pomatoschistus Microps: Linking Biomarkers to Behaviour. *Chemosph.* **2009**, *76*, 1416–1427.
2. Buikema, A. L., Jr.; Niederlehner, B. R.; Cairns, J. K., Jr. Biological Monitoring. Part IV. Toxicity Testing. *Water Res.* **1982**, *16*, 239–262.
3. Sprague, J. B. Measurement of Pollutant Toxicity to Fish I. Bioassay Methods for Acute Toxicity. *Water Res.* **1969**, *3*, 793–821.
4. Farré, M.; Barceló, D. Toxicity Testing of Wastewater and Sewage Sludge by Biosensors, Bioassays and Chemical Analysis. *Trends Anal. Chem.* **2003**, *22*, 299–310.
5. Parvez, S.; Venkataraman, C.; Mukherji, S. A Review on Advantages of Implementing Luminescence Inhibition Test (*Vibrio fischeri*) for Acute Toxicity Prediction of Chemicals. *Environ. Int.* **2006**, *32*, 265–268.
6. Mallouk, T. E.; Sen, A. Powering Nanorobots. *Sci. Am.* **2009**, *300*, 72–77.

7. Wang, J. Can Man-Made Nanomachines Compete with Nature Biomotors? *ACS Nano* **2009**, *3*, 4–9.
8. Mirkovic, T.; Zacharia, N. S.; Scholes, G. D.; Ozin, G. A. Fuel for Thought: Chemically Powered Nanomotors Out-Swim Nature's Flagellated Bacteria. *ACS Nano* **2010**, *4*, 1782–1789.
9. Pumera, M. Electrochemically Powered Self-Propelled Electrophoretic Nanosubmarines. *Nanoscale* **2010**, *2*, 1643–1649.
10. Wang, J.; Gao, W. Nano/Microscale Motors: Biomedical Opportunities and Challenges. *ACS Nano* **2012**, *6*, 5745–5751.
11. Mei, Y. F.; Solovev, A. A.; Sanchez, S.; Schmidt, O. G. Rolled-up Nanotech on Polymers: From Basic Perception to Self-Propelled Catalytic Microengines. *Chem. Soc. Rev.* **2011**, *40*, 2109–2119.
12. Mei, Y. F.; Huang, G. S.; Solovev, A. A.; Urena, E. B.; Monch, I.; Ding, F.; Reindl, T.; Fu, R. K. Y.; Chu, P. K.; Schmidt, O. G. Versatile Approach for Integrative and Functionalized Tubes by Strain Engineering of Nanomembranes on Polymers. *Adv. Mater.* **2008**, *20*, 4085–4090.
13. Gao, W.; Sattayasamitsathit, S.; Orozco, J.; Wang, J. Highly Efficient Catalytic Microengines: Template Electrosynthesis of Polyaniline/Platinum Microtubes. *J. Am. Chem. Soc.* **2011**, *133*, 11862–11864.
14. Balasubramanian, S.; Kagan, D.; Hu, C. J.; Campuzano, S.; Lobo-Castañ̃o, M. J.; Lim, N.; Kang, D. Y.; Zimmerman, M.; Zhang, L.; Wang, J. Micromachine-Enabled Capture and Isolation of Cancer Cells in Complex Media. *Angew. Chem., Int. Ed.* **2011**, *50*, 4161–4164.
15. Campuzano, S.; Orozco, J.; Kagan, D.; Guix, M.; Gao, W.; Sattayasamitsathit, S.; Claussen, J. C.; Merkoci, A.; Wang, J. Bacterial Isolation by Lectin-Modified Microengines. *Nano Lett.* **2012**, *12*, 396–401.
16. Huang, G. S.; Wang, J.; Mei, Y. F. Material Considerations and Locomotive Capability in Catalytic Tubular Microengines. *J. Mater. Chem.* **2012**, *22*, 6519–6525.
17. Sanchez, S.; Solovev, A. A.; Mei, Y. F.; Schmidt, O. G. Dynamics of Biocatalytic Microengines Mediated by Variable Friction Control. *J. Am. Chem. Soc.* **2010**, *132*, 13144–13145.
18. Gao, W.; Sattayasamitsathit, S.; Uygun, A.; Pei, A.; Ponedal, A.; Wang, J. Polymer-Based Tubular Microbots: Role of Composition and Preparation. *Nanoscale* **2012**, *4*, 2447–2453.
19. Kagan, D.; Laocharoensuk, R.; Zimmerman, M.; Clawson, C.; Balasubramanian, S.; Kang, D.; Bishop, D.; Sattayasamitsathit, S.; Zhang, L.; Wang, J. Rapid Delivery of Drug Carriers Propelled and Navigated by Catalytic Nanoshuttles. *Small* **2010**, *6*, 2741–2747.
20. Campuzano, S.; Kagan, D.; Orozco, J.; Wang, J. Motion-Driven Sensing and Biosensing Using Electrochemically Propelled Nanomotors. *Analyst* **2011**, *136*, 4621–4630.
21. Guix, M.; Orozco, J.; Garcia, M.; Gao, W.; Sattayasamitsathit, S.; Merkoci, A.; Escarpa, A.; Wang, J. Superhydrophobic Alkanethiol-Coated Microsubmarines for Effective Removal of Oil. *ACS Nano* **2012**, *6*, 4445–4451.
22. Zhao, G. J.; Seah, T. H.; Pumera, M. External-Energy-Independent Polymer Capsule Motors and Their Cooperative Behaviors. *Chem.—Eur. J.* **2011**, *17*, 12020–12026.
23. Sole, S.; Merkoci, A.; Alegret, S. *Crit.* Determination of Toxic Substances Based on Enzyme Inhibition. Part I. Electrochemical Biosensors for the Determination of Pesticides Using Batch Procedures. *Crit. Rev. Anal. Chem.* **2003**, *33*, 89–126.
24. Trojanowicz, M. Determination of Pesticides Using Electrochemical Enzymatic Biosensors. *Electroanal.* **2002**, *14*, 1311–1328.
25. Amine, A.; Mohammadi, H.; Bourais, I.; Palleschi, G. Enzyme Inhibition-Based Biosensors for Food Safety and Environmental Monitoring. *Biosens. Bioelectron.* **2006**, *21*, 1405–1423.
26. Wang, J.; Nascimento, V. G.; Kane, S. A.; Rogers, K.; Smyth, M. R.; Agnes, L. Screen-Printed Tyrosinase-Containing Electrodes for the Biosensing of Enzyme Inhibitors. *Talanta* **1996**, *43*, 1903–1907.
27. Sezgintürk, M. K.; Göktuğ, T.; Dinçkaya, E. A Biosensor Based on Catalase for Determination of Highly Toxic Chemical Azide in Fruit Juices. *Biosens. Bioelectron.* **2005**, *21*, 684–688.
28. Vasylkiv, O. Y.; Kubrak, O. I.; Storey, K. B.; Lushchak, V. I. Catalase Activity as a Potential Vital Biomarker of Fish Intoxication by the Herbicide Aminotriazole. *Pestic. Biochem. Physiol.* **2011**, *101*, 1–5.
29. Singh, S. M.; Sivalingam, P. M. *In Vitro* Study on the Interactive Effects of Heavy Metals on Catalase Activity of *Sarotherodon mossambicus* (Peters). *J. Fish Biol.* **1982**, *20*, 683–688.
30. Margoliash, E.; Novogrodsky, A.; Schejter, A. Irreversible Reaction of 3-Amino-1:2:4-triazole and Related Inhibitors with the Protein of Catalase. *Biochem. J.* **1960**, *74*, 339–348.
31. Manesh, K. M.; Cardona, M.; Yuan, R.; Kagan, D.; Balasubramanian, S.; Wang, J. Template-Assisted Fabrication of Salt-Independent Catalytic Tubular Microengines. *ACS Nano* **2010**, *4*, 1799–1804.